Neovascularization of poly(ether ester) block-copolymer scaffolds *in vivo*: Long-term investigations using intravital fluorescent microscopy

Daniel Druecke,[1]* Stefan Langer,[1]* Evert Lamme,[2] Jeroen Pieper,[2] Marija Ugarkovic,[1] Hans Ulrich Steinau,[1] Heinz Herbert Homann[1]

[1]*Department for Plastic and Hand Surgery/Burn Center, Ruhr University Bochum, Buerkle-de-la-Camp Platz 1, 44789 Bochum, Germany*

[2]*ISOTIS NV, Bilthoven, The Netherlands*

Received 17 January 2003; revised 23 May 2003; accepted 24 June 2003

Abstract: Poly(ether ester) block-copolymer scaffolds of different pore size were implanted into the dorsal skinfold chamber of balb/c mice. Using intravital fluorescent microscopy, the temporal course of neovascularization into these scaffolds was quantitatively analyzed. Three scaffold groups (diameter, 5 mm; 220–260 thickness, μm; $n = 30$) were implanted. Different pore sizes were evaluated: small (20–75 μm), medium (75–212 μm) and large pores (250–300 μm). Measurements were performed on days 8, 12, 16, and 20 in the surrounding normal tissue, in the border zone, and in the center of the scaffold. Standard microcirculatory parameters were assessed (plasma leakage, vessel diameter, red blood cell velocity, and functional vessel density). The large-pored scaffolds showed significantly higher functional vessel density in the border zone and in the center (days 8 and 12) compared with the scaffold with the small and medium-sized pores. These data correlated with a larger vessel diameter and a higher red blood cell velocity in the large-pored scaffold group. Interestingly, during the evaluation period the microcirculatory parameters on the edge of the scaffolds returned to values similar to those found in the surrounding tissue. In the center of the scaffold, however, neovascularization was still active 20 days after implantation. Plasma leakage and vessel diameter were higher in the center of the scaffold. Red blood cell velocity and functional vessel density were 50% lower than in the surrounding tissue. In conclusion, the dorsal skinfold chamber model in mice allows long-term study of blood vessel growth and remodeling in porous biomedical materials. The rate of vessel ingrowth into poly(ether ester) block-copolymer scaffolds is influenced by pore size and was highest in the scaffold with the largest pores. The data generated with this model contribute to knowledge about the development of functional vessels and tissue ingrowth into biomaterials. © 2003 Wiley Periodicals, Inc. J Biomed Mater Res 68A: 10–18, 2004

Key words: biomaterials; block-copolymer scaffolds; intravital microscopy; microcirculation; mouse skinfold chamber; neovascularization; tissue engineering

INTRODUCTION

The technique of tissue engineering involves the replacement of diseased, injured, or missing body tissues with biologically compatible "living" substitutes. However, after transfer *in vivo*, such tissue substitutes are not able to survive by diffusion alone.[1] To prevent mass loss of engineered tissue, the initial ischemic time window should be as small as possible. Thus, it is well known that rapid ingrowth of blood vessels is the prerequisite for survival, and biomedical materials used in tissue engineering should support or stimulate rapid ingrowth. New vessels in biomaterials are formed from existing blood vessels from surrounding host tissue through sprouting, a process termed "angiogenesis."[2]

Poly(ether ester) block-copolymer biomaterials are currently in use in wound healing, as well as in the field of cartilage and bone replacement. In wound healing, porous scaffolds were used as a dermal regeneration template[3] and as a cell-seeded skin substitute for the treatment of deep skin defects.[4–7] In bone substitution, the copolymer has shown osteoconductive and bone-bonding characteristics.[8,9] Poly(ether ester) block-copolymer scaffold implants can be easily tailored, are biodegradable, and have proven to support ingrowth of different tissues. It has previously been shown that pore size and void fraction (porosity)

*Both authors contributed equally to the study.

Correspondence to: S. Langer; e-mail: Stefan.Langer@ruhr-uni-bochum.de

Contract grant sponsor: ISOTIS NV, The Netherlands

of biomedical materials control the rate and depth of cellular ingrowth.[10]

However, data on the temporal course of neovascularization of poly(ether ester) block-copolymer biomaterials are scarce. This is due mainly to the paucity of animal models allowing quantitative analysis of vascular ingrowth into biomaterials. Therefore, the aim of the current study was to investigate whether the skinfold chamber in mice could be used to quantify the process of neovascularization into poly(ether ester) block-copolymer scaffold over time using intravital fluorescent microscopy.

MATERIALS AND METHODS

Animal model

The dorsal skinfold chamber (Fig. 1) in conscious female balb/c mice (n = 30) was used as the model to perform microvascular measurements in poly(ether ester) block-copolymer scaffolds. The animals, purchased from Charles River (Sulzfeld, Germany), were 4–5 weeks old and had a body weight of 22–25 g. The mice were kept at 21°C in a normal 12/12-h light/dark circle and fed laboratory diet (Sniff, Soest, Germany) and tap water *ad libitum.* The experiments were conducted in accordance with German animal protection law.

Surgical procedure

The chambers and the microsurgical implantation used in the study are based on the report of Endrich et al.,[11] with only a few minor modifications. Briefly, the mice were anesthetized by i.m. injection of ketamine (100 mg/kg body weight; Ketavet, Parke-Davis, Berlin, Germany) and xylazine 2% (10 mg/kg body weight; Rompun, Bayer, Leverkusen, Germany). The hair was removed chemically from the animals' backs (Pilca Med, Olivia, Hamburg, Germany). An extended double layer of skin of the dorsal skinfold was sandwiched between two symmetrical titanium frames. The distance between the two titanium frames was set to 400–450 μm. A circular area of 15 mm in diameter from one layer of skin was completely removed. The remaining layers of the other skinfold (thin striated skin muscle, subcutaneous tissue, dermis, and epidermis) were covered with a glass coverslip incorporated into one of the titanium frames. The titanium chambers were purchased from the Institute for Surgical Research, Ludwig-Maximilians University, Munich, Germany. All surgical procedures were performed under sterile conditions. The animals tolerated the chamber very well and showed no signs of discomfort (eating and sleeping habits were unaltered). The dorsal skinfold chamber is a widely used and well-accepted model in microcirculatory research in hamsters and mice.[12–18]

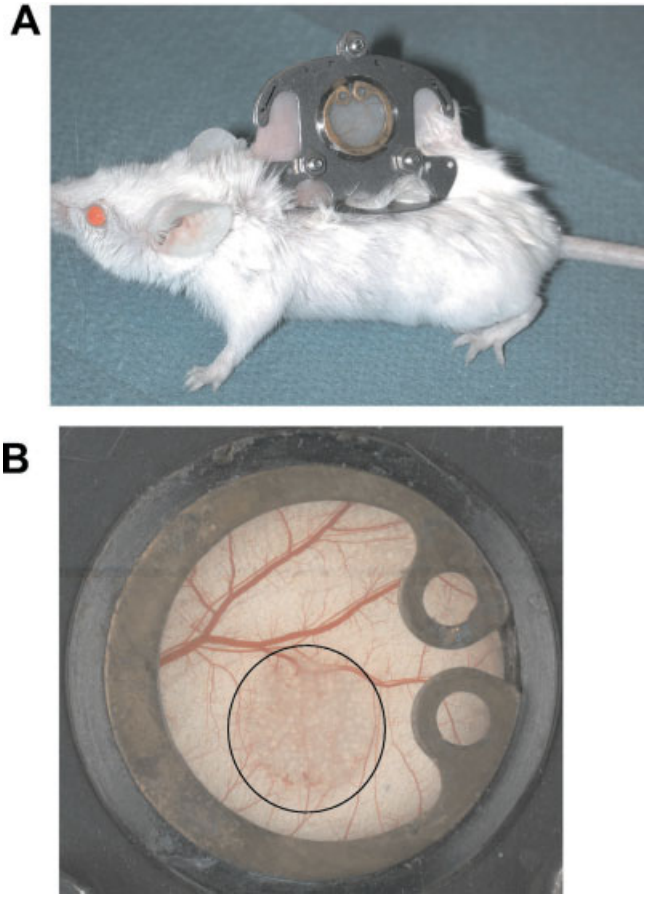

Figure 1. Illustration of the skinfold chamber model in a mouse (A). At higher magnification (B) the poly(ether ester) block–copolymer scaffold implanted onto the striated muscle in the chamber (marked with black circle) can be identified by transillumination. Scaffold as well as the microcirculation of the chamber can be observed through a cover glass. [Color figure can be viewed in the online issue, which is available at www.interscience.wiley.com.]

Scaffold manufacturing and characteristics

A block-copolymer polymer composed of alternating soft blocks of polyethylene glycol terephthalate (PEGT) and hard blocks of polybutylene terephthalate (PBT) was used. Polymer composition can be modified by varying the weight percentages of PEGT and PBT or by changing the molecular weight (MW) of the PEG. The scaffolds used in the current study were produced by solvent-casting, particulate-leaching[19] using a copolymer with a composition PEGT/PBT weight ratio of 55/45 and PEG MW of 300 (300PEGT55/PBT45). This composition supported the growth of fibroblasts and keratinocytes.[20] The scaffolds were circular, with a diameter of 5 mm and a thickness of 220–260 μm and a porosity of 70–80%. Pore size was varied with the following diameters: group 1, 20–75 μm; group 2, 75–212 μm, group 3, 250–300 μm. Scaffold morphology from both sides of the scaffold is shown in Figure 2 using standard SEM analysis. After preparation, the scaffolds were single-packed, randomized, and labeled. The scaffolds were sterilized using

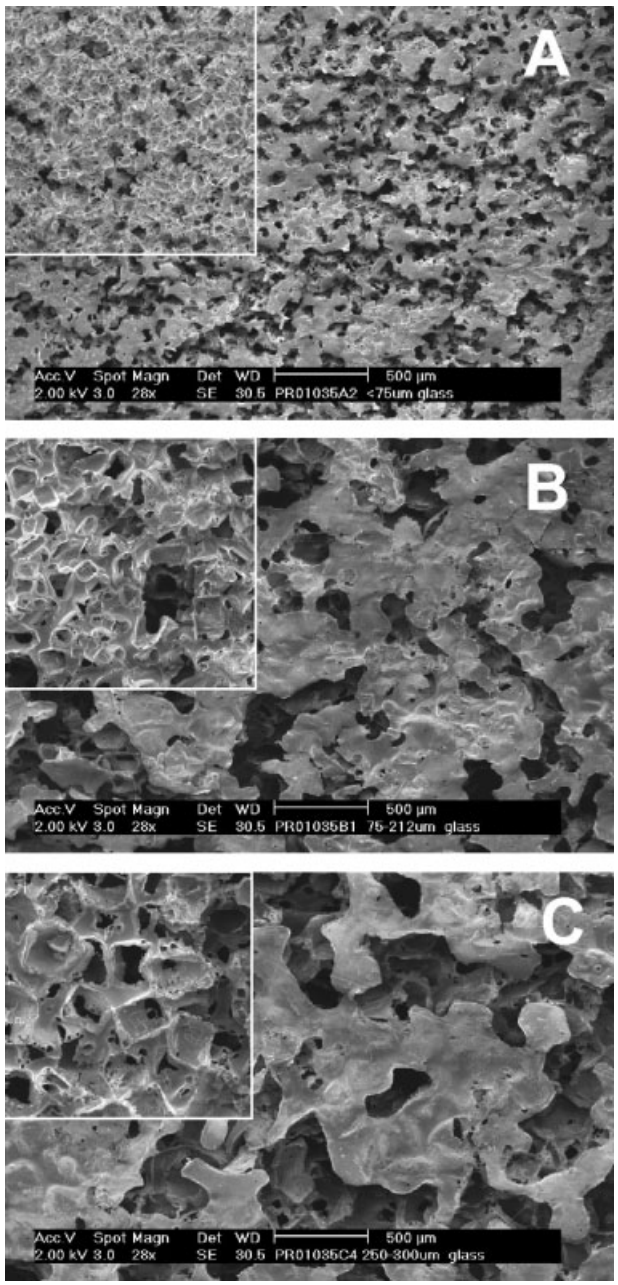

Figure 2. The structure of the porous poly(ether ester) block–copolymer scaffolds as imaged by electron microscopy. Three different types of scaffolds (A: 20–75 μm; B: 75–212 μm, C: 250–300 μm) were implanted into the chamber to measure neovascularization.

steam sterilization (121°C for 10 min) and stored in the dark at −20°C prior to implantation.

Scaffold implantation and intravital fluorescent microscopy (IFM)

The mice were anesthetized once again 48 h after chamber preparation. When microcirculation in the chamber was intact, the cover glass of the chamber was removed and a single scaffold was transferred onto the striated muscle of the opposing skinfold (Figs. 1 and 3). The chamber was closed with a new, sterile cover glass. Special care was taken to avoid desiccation of the tissues.

Neovascularization was assessed in the surrounding tissue (I, control tissue), the border zone of the scaffold (II), and in the center of the scaffold [III; Fig. 3(B)]. The mice were immobilized in a plexiglass tube and the chamber was attached to the microscope stage of the IFM setup. The setup permits repeated scanning of identical tissue areas containing microvessels. A 20-fold water immersion objective (Zeiss, Axiotech Vario 100 HD, Acroplan 20X0.5 W, Zeiss, Oberkochen, Germany) was used to observe the microvessels. The total on-screen magnification was 533-fold. To avoid observer bias, measurements were made after zooming into the scaffold. In the case that vessels were found, the microcirculation was videotaped. For the IFM measurements, 0.05 mL of Ringer's solution containing 5% fluorescein isothiocyanate–labeled dextran (FITC-dextran, MW 150.000; Sigma Chemicals Co., St. Louis, MO) was injected for contrast enhancement via a tail vein. The images [Figure 3(C)] were captured using a charge coupled device video camera and recorded on SVHS videotapes (Sony, Cologne, Germany) for subsequent off-line analysis. Epi-illumination was achieved using a 12-V, 100-W halogen lamp in conjunction with a Zeiss filter set (excitation 450–490 nm, emission $>$ 510 nm).

In each area, five different microvascular regions of interest (ROIs) were selected, recorded on videotape, and their positions outlined using a schematic drawing so that it was possible to relocate the exact ROIs. Measurements were performed 8, 12, 16, and 20 days after scaffold implantation. At the end of the protocol, the animals were killed under isoflurane anesthesia by an overdose of pentobarbital. The implants were harvested for routine histological processing and examination [hematoxylin and eosin (H&E) staining; data not shown).

Data acquisition

Analysis of the videotapes was performed off-line using the commercially available CapImage® computer program (Dr. Zeintl, Heidelberg, Germany).[21] The following parameters were assessed: macromolecular leakage of the plasma marker FITC-dextran from vessels (Ii/Io), vessel diameter (μm), midstream red blood cell velocity (RBCV) in the vessels (mm/s), and functional vessel density (FVD) (cm/cm^2).

Leakage of the plasma marker FITC-dextran 150.000 from vessels is a measure of vessel maturation.[22] It is calculated as the ratio between the fluorescence intensity measured inside versus outside a vessel. Diameter measurements provide information about changes of local microangiodynamics, for example, during ischemia/reperfusion or wound healing.[23] Functional capillary density is measured as the length of vessels perfused by red blood cells per observed area. This parameter is used as an index for tissue perfusion and tissue oxygenation.[24,25] the parameter RBCV is used for microvascular properties and can be influenced by chemotactic accumulation and adhesion of leukocytes, for example.[26]

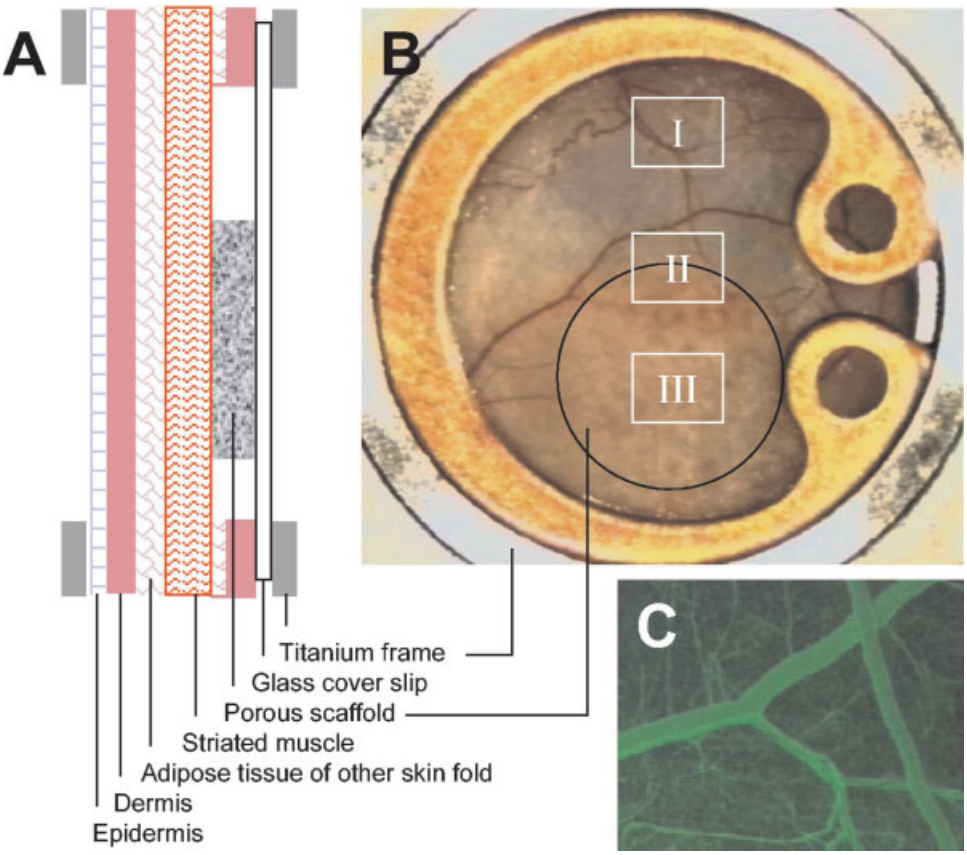

Figure 3. (A) Schematic drawing of a cross-section through the chamber preparation . (B) Different sites of interest in which the microcirculation was assessed (I, host tissue; II, border zone of the scaffold; III, center of the scaffold). (C) Typical microvessels of the surrounding host tissue (stained with FITC-dextran 150,000) as visualized by means of IFM. [Color figure can be viewed in the online issue, which is available at www.interscience.wiley.com.]

Statistics

The study was performed single-blinded. Comparison between groups was performed using the Kruskal–Wallis one-way analysis of variance on ranks test. When significant differences were found, a pairwise multiple-comparison procedure (Dunn's method) was carried out. Data are given in mean ± SEM. A p-value less than 0.05 was regarded as statistically significant. A commercially available software package (Sigma Stat, SPSS Inc., version 2.03) was used to calculate significance.

RESULTS

Using the skinfold chamber model in mice, it was possible to perform long-term, quantitative *in vivo* assessment of neovascularization of poly(ether ester) block-copolymer scaffolds. The IFM measurements were possible using porous scaffolds with a thickness of less than 300 μm. In Figure 4, typical IFM images videotaped in the center of one scaffold are shown. Neovascularization within these scaffolds can be clearly identified. From these images the quantitative analysis was performed.

As expected, in the surrounding host tissue (control tissue) all measured microcirculatory parameters (leakage of the plasma marker, vessel diameter, RBCV, and FVD) remained stable throughout the observation period.

In the border zone of all scaffolds used, plasma leakage was comparable to that in the surrounding tissue (Fig. 5), indicating a mild inflammatory response/foreign body reaction to the implant. In the center of the scaffold, however, leakage was significantly higher than in the surrounding tissue, indicating reduced integrity of endothelial cells in the area.

The average vessel diameter in the surrounding tissue was approx. 6.5 μm. At the edge of the scaffold, the vessel diameter was significantly higher than in the surrounding tissue and decreased from approximately 13 μm to approximately 10 μm during the evaluation period (Fig. 6). After 8 and 12 days, at the edge of scaffolds a trend toward blood vessels with a larger diameter in the scaffold with the larger pores was observed. The difference between scaffolds with

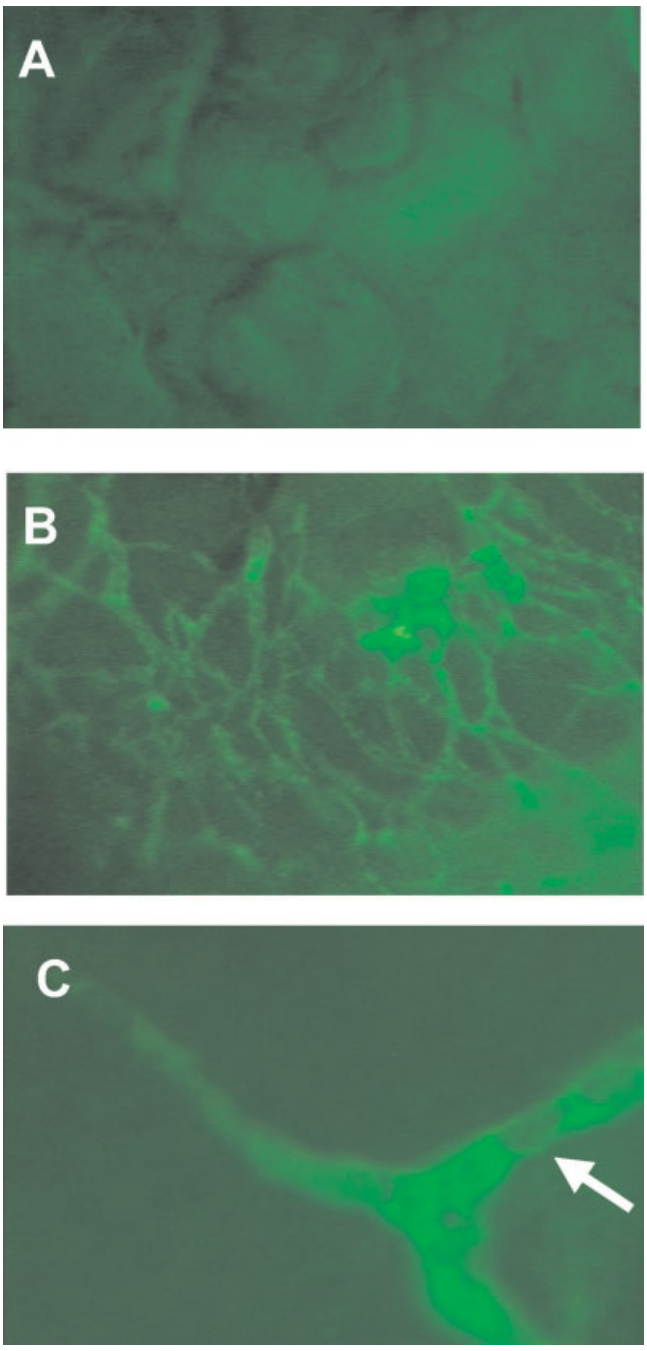

Figure 4. Poly(ether ester) block-copolymer scaffold as imaged by intravital microscopy: (A) Microvessels were not detected in scaffolds immediately after implantation. The porous structure of the scaffold becomes apparent. Neovascularization within implants after application of the plasma marker FITC-dextran in the border zone of the implant. (B) Vessel morphology is tortous, dilated, and not organized (day 20; original magnification ×50). (C) Vessel sprouts and red blood cells (white arrow) within the vessels can be videotaped at higher magnification (day 8; original magnification ×533). The setup allows for return to the identical vessel at subsequent time points to perform long-term investigation of the same site of interest in the microcirculation. [Color figure can be viewed in the online issue, which is available at www.interscience.wiley.com.]

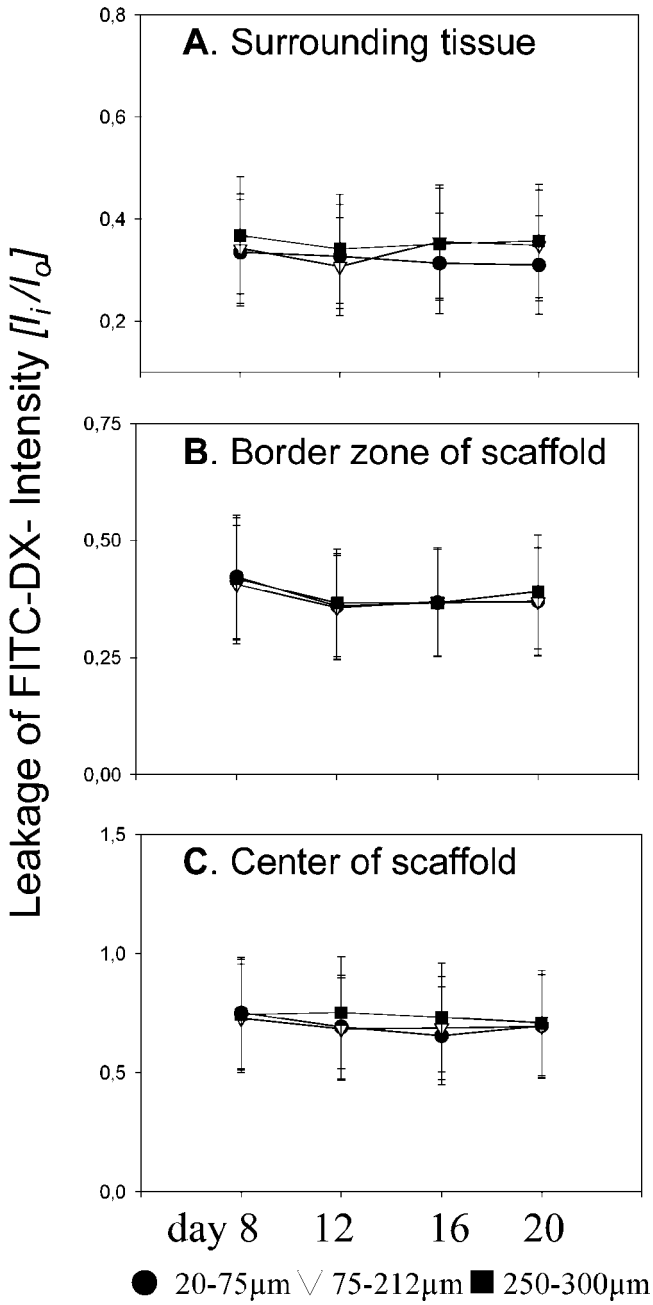

Figure 5. The quantitative data of FITC-dextran leakage from the microvessels into the surrounding tissue. Leakage in the scaffold border zone was similar to that in surrounding tissue. Leakage was stable in all tissues over time, and no differences between the groups were observed. Leakage in the center of the scaffolds was higher in all groups as compared with host tissue and border zone.

the smallest and the largest pores (10.11 ± 0.7 vs 13.8 ± 0.8) was significant. After 8 days, vessel diameter in the center of the scaffolds was also significantly larger in the scaffolds with largest pores than in those with the smallest pores. In the center, vessel diameter remained constant during the evaluation period but was significantly larger than in the surrounding tissue.

The velocity of red blood cells in the vessel, 0.2–0.3

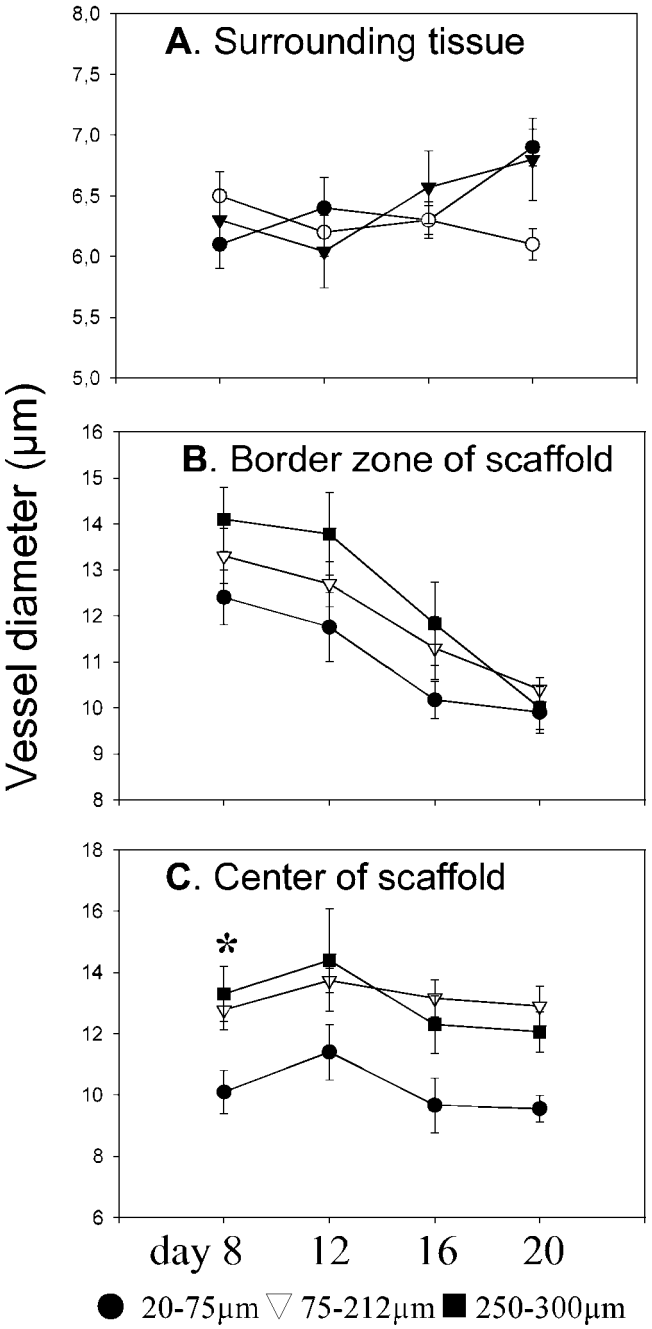

Figure 6. Vessel diameter decreased over time at border zone of the scaffold. Largest diameters were measured in the large-pore scaffold group.

mm/s, was similar in the surrounding tissue and at the edge of the scaffolds from day 8 until day 20 (Fig. 7). After 8 and 12 days, the RBCV in the center of the scaffolds was significantly higher in the scaffold with the largest pores. With increasing time, the average velocity increased in the scaffolds with the small and medium-sized pores to the same velocity as in the scaffolds with the large pores. Nevertheless, the RBCV in the center of the scaffold was significantly (approximately 50%) lower than in vessels in the surrounding tissue and at the edge of the scaffold.

In the surrounding tissue, the FVD was between 220 and 240 cm/cm^2 (Fig. 8). At the edge of the scaffold after 8 days, the FVD was significantly higher for the scaffolds with the largest pores. At this point in time, the FVD was relatively low (50–100 cm/cm^2) but increased over time in all scaffold groups, to reach the same level as in the surrounding tissue at day 20. In the center of the scaffolds, after 8 and 12 days, the FVD was significantly higher in the scaffold with the large pores. Over the time period of observation, the FVD increased in all groups

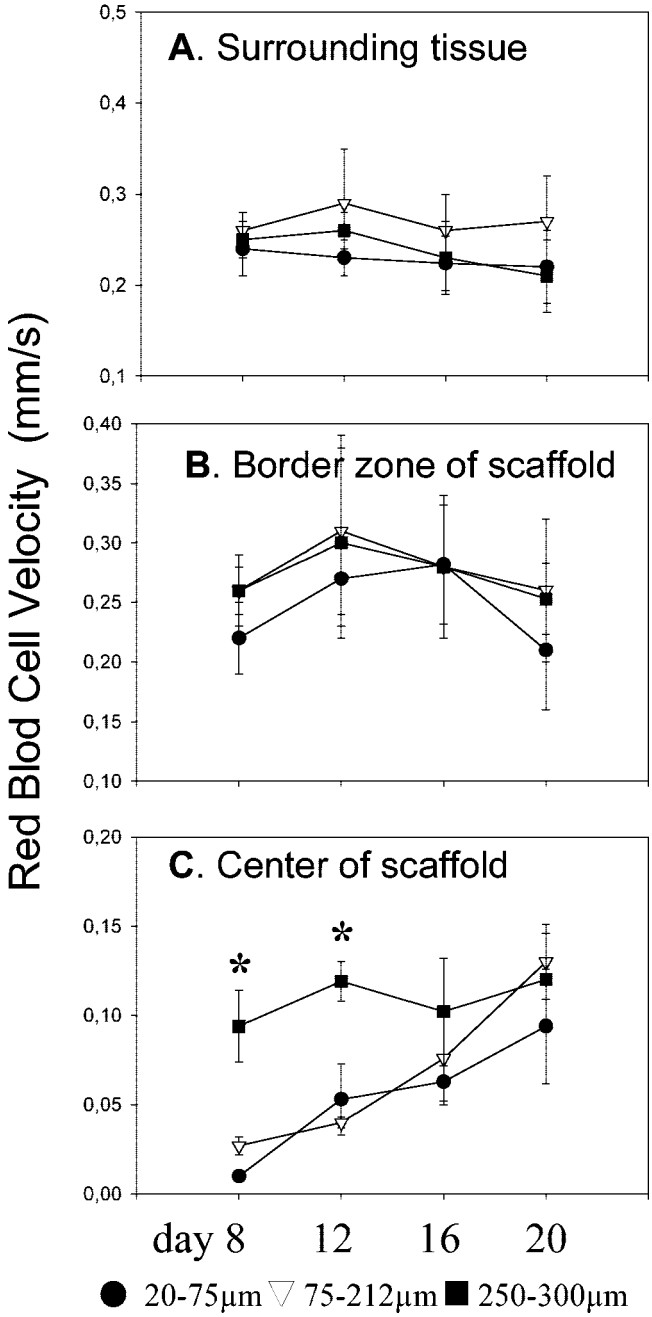

Figure 7. The RBCV was constant in surrounding tissue and border zone of the scaffold. Significantly higher RBCV in the center of the scaffold was found in 250–300-µm scaffolds.

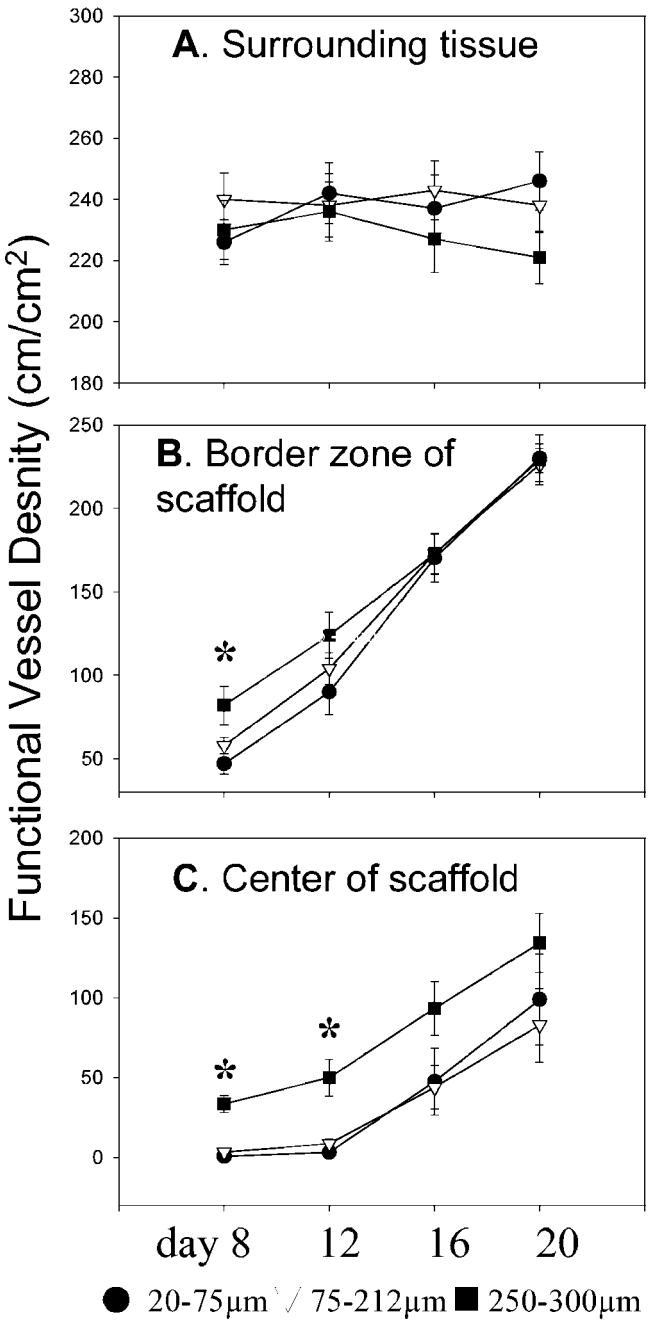

Figure 8. The FVD increased in all groups at the border zone of the scaffolds. In the center of the scaffolds, the 250–300-μm group showed significantly higher FVD on days 8 and 12.

from 0–40 to 70–150 cm/cm,^{2} but did not reach the same level as in the surrounding tissue.

DISCUSSION

Knowledge about the influence of biomaterial modifications and its effect on neovascularization is an important issue in the field of tissue engineering, with one goal being the improvement of product efficiacy.[27–29] Data on neovascularization of biomaterials are based today mainly on semiquantitative histological studies.[10,19,29,30] The dynamic temporal course of neovascularization was previously evaluated by means of magnetic resonance imaging techniques in animals[31] as well as in humans.[32] Using a corneal micropocket model, angiogenesis into biodegradable hydrogel implant could be assessed over long time by means of biomicroscopy.[33]

We have demonstrated that the skinfold chamber model in mice is an adequate model to accurately measure the process of neovascularization into copolymer scaffolds *in vivo.* The model thus allows repeated quantitative assessment of one major characteristic of a living biomaterial: its vascular network.

After insertion of porous block copolymers, the key parameters of microcirculation in the surrounding control tissue (striated skin muscle) remained constant, comparable to data gathered in previous studies using the same model.[22,34] This can be interpreted as proof of the stability of the model used. The model also allows evaluation of inflammatory/foreign body response to the scaffold material.

Inflammation is known to increase leakage of FITC-dextran out of the microcirculation.[22] In the current study, using scaffolds prepared with the block copolymer PEGT and PBT, FITC-dextran leakage at border zone of the scaffolds was similar to that in the surrounding tissue. This can be interpreted as an absence of inflammatory reaction to the biomaterial used. A trend was observed when scaffolds with a similar morphology but an increased average pore diameter were used inasmuch as larger pore diameters were associated with higher FVD. This trend was also previously observed in investigations of fibrovascular tissue ingrowth into amorphous poly(L-lactic acid) scaffolds.[10] In the study, optimal ingrowth was measured in scaffolds with a pore size of 500 μm. In contrast, because of the model used in the current study, scaffold thickness was limited to a thickness of 300 μm, allowing evaluation of scaffolds with a maximal diameter of 250–300 μm. Moreover, increased scaffold material volumes also interfere with fluorescent image resolution.

Interestingly, after 8 days, vessel diameter in the border zone of the scaffold was much larger than in the surrounding tissue and decreased over time to the same value as that found in the surrounding tissue. At the same time, when vessel diameter decreased, FVD increased to values similar to those found in the surrounding tissue.

The IFM data were different in the center of the scaffold. Plasma leakage was higher than at the edge and in the surrounding tissue, vessel diameter increased, and RBCV and FVD were lower during the entire evaluation period. Apparently new and imma-

ture vessels continued to be formed or remodeled in this part of the scaffold. Moreover, in this area vessel morphology was still unsystematic and twisted but, in contrast, was well organized, with a parallel orientation in the surrounding tissue.

The time required for scaffold neovascularization as found in the current study appears to be excessive. The degree of neovascularization of the scaffolds measured at day 20 was not comparable to that of surrounding muscle. The ischemic period of the scaffolds after their transfer was too long to serve as an ideal scaffold for tissue engineering. However, the same type of scaffold was previously used in rats and pigs and showed more rapid tissue ingrowth compared with our skinfold model. The differences may be explained in part by the greater rate of healing response in rats and pigs as well as by the exposure of tissue to air.[3,5] Migrating keratinocytes in the epidermis produce angiogenesis stimulating factors (e.g., vascular endothelial growth factor, keratinocyte growth factor). In the skinfold model the scaffolds were implanted into a closed chamber under a cover glass, which explains the differences between the data sets.

Transplantation of autologous adipose tissue in a skinfold model in hamsters showed vascular sprouts in the border zone 1 day after transplantation.[17] Interestingly, the FVD in the adipose tissue was always higher in the border zone of the graft when compared with the center. After 3 weeks of observation, the FVD data at the border zone and in the center were comparable to the FVD data of the poly(ether ester) block-copolymer scaffolds used in the current study.

The skinfold model in combination with IFM was previously used in hamsters to study biomaterials and their vascular networks.[15,17,35] A biosynthetic collagen/polyester material showed a higher FVD as compared with polytetrafluorethylene synthetic material. It should be noted that the scaffold dimensions in that study ($1 \times 1 \times 1$ mm) differed from the dimensions used in our study. For the synthetic scaffold, this value was reached only after 20 days. Apparently, tissue ingrowth into synthetic materials can still be accelerated, and different strategies can be followed, for example, via biomaterial surface modification, release of hormones and/or peptides, or the presence of cells in the material. For example, one of the more promising methods seems to include endothelial cells or chondrocytes into such biomaterials.[36,37] In a study by Nor and coworkers,[38] human endothelial cells on porous poly lactide matrices (average diameter, 250 μm) were transferred into immunodeficient mice. Nonfunctional tubular structures were found 5 days after implantation and as early as 7–10 days subsequent to implantation blood cells were detected in the vessels using histochemical methods. Interestingly, the authors not only demonstrated endothelial vessel differentiation into functional vessels, but human endothelial vessels were characterized by anastomoses with mouse vasculature.

In conclusion, the skinfold chamber in mice can be used to study the mechanisms of neovascularization into biomaterials and contributes to a better understanding of the interactions between biomaterial surfaces and host tissues. The poly(ether ester) block-copolymer scaffolds with the largest pores showed significantly more rapid vessel ingrowth and maturation as compared with scaffolds with smaller pores. However, scaffold vascularization in the center of the scaffolds did not reach the level found in the surrounding tissue. A foreign body reaction of the used poly(ether ester) block-copolymer scaffolds to the surrounding host tissue did not take place.

Future study will be directed toward enhancement of neovascularization by the use of slow-release actives from the biomaterial. The influence of seeded and culture cells on neovascularization of porous poly(ether ester) block-copolymer scaffolds should also be investigated.

The microcirculatory laboratory in which the research was performed is supported by the Vogelsang Foundation, Bochum and Philoktet e.V., Bochum, Germany. This work is part of the doctoral thesis of M. Ugarkovic and A. Ring.

References

1. Folkman J. Angiogenesis in cancer, vascular, rheumatoid and other disease. Nat Med 1995;1:27–31.
2. Carmeliet P. Mechanisms of angiogenesis and arteriogenesis. Nat Med 2000;6:389–395.
3. Beumer GJ, van Blitterswijk CA, Ponec M. Degradative behaviour of polymeric matrices in (sub)dermal and muscle tissue of the rat: a quantitative study. Biomaterials 1994;15:551–559.
4. Beumer GJ, van Blitterswijk CA, Bakker D, Ponec M. A new biodegradable matrix as part of a cell seeded skin substitute for the treatment of deep skin defects: a physico-chemical characterisation. Clin Mater 1993;14:21–27.
5. Van Dorp AG, Verhoeven MC, Koerten HK, Van Der Nat-Van Der Meij TH, Van Blitterswijk CA, Ponec M. Dermal regeneration in full-thickness wounds in Yucatan miniature pigs using a biodegradable copolymer. Wound Repair Regen 1998;6:556–68.
6. Xiao YRJ, van Blitterswijk CA. Static and dynamic fibroblast seeding and cultivation in porous PEO/PBT scaffolds. J Mater Sci Mater Med 1999;10:773–777.
7. Radder AM, Leenders H, van Blitterswijk CA. Application of porous PEO/PBT copolymers for bone replacement. J Biomed Mater Res 1996;30:341–51.
8. Bulstra SK, Geesink RG, Bakker D, Bulstra TH, Bouwmeester SJ, van der Linden AJ. Femoral canal occlusion in total hip replacement using a resorbable and flexible cement restrictor. J Bone Joint Surg Br 1996;78:892–898.
9. van Loon JALH, Goedemoed JH, van Blitterswswijk CA. Tissue reaction during long term implantation in relation to degradation. A study of range of PEO/PBT copolymers. 20th Annual Meeting of the Society of Biomaterials 1994. p 370.
10. Wake MC, Patrick CW Jr, Mikos AG. Pore morphology effects on the fibrovascular tissue growth in porous polymer substrates. Cell Transplant 1994;3:339–343.

11. Endrich B, Asaishi K, Gotz A, Messmer K: Technical report—a new chamber technique for microvascular studies in unanesthetized hamsters. Res Exp Med (Berlin) 1980;177:125–134.
12. Harris AG, Steinbauer M, Leiderer R, Messmer K. Role of leukocyte plugging and edema in skeletal muscle ischemia–reperfusion injury. Am J Physiol 1997;273:H989–H996.
13. Langer S, Abels C, Botzlar A, Pahernik S, Rick K, Szeimies RM, Goetz AE. Active and higher intracellular uptake of 5-aminolevulinic acid in tumors may be inhibited by glycine. J Invest Dermatol 1999;112:723–728.
14. Lehr HA, Leunig M, Menger MD, Nolte D, Messmer K. Dorsal skinfold chamber technique for intravital microscopy in nude mice. Am J Pathol 1993;143:1055–1062.
15. Menger MD, Hammersen F, Walter P, Messmer K. Neovascularization of prosthetic vascular grafts. Quantitative analysis of angiogenesis and microhemodynamics by means of intravital microscopy. Thorac Cardiovasc Surg 1990;38:139–145.
16. Sakai H, Hara H, Tsai AG, Tsuchida E, Intaglietta M. Constriction of resistance arteries determines l-NAME–induced hypertension in a conscious hamster model. Microvasc Res 2000;60: 21–27.
17. Langer S, Sinitsina I, Biberthaler P, Krombach F, Messmer K. Revascularization of transplanted adipose tissue: a study in the dorsal skinfold chamber of hamsters. Ann Plast Surg 2002;48: 53–59.
18. Menger MD, Hammersen F, Messmer K. *In vivo* assessment of neovascularization and incorporation of prosthetic vascular biografts. Thorac Cardiovasc Surg 1992;40:19–25.
19. Deodato B, Arsic N, Zentilin L, Galeano M, Santoro D, Torre V, Altavilla D, Valdembri D, Bussolino F, Squadrito F, Giacca M. Recombinant AAV vector encoding human VEGF165 enhances wound healing. Gene Ther 2002;–9:777–785.
20. van Dorp AG, Verhoeven MC, Koerten HK, van Blitterswijk CA, Ponec M. Bilayered biodegradable poly(ethylene glycol)/poly(butylene terephthalate) copolymer (Polyactive) as substrate for human fibroblasts and keratinocytes. J Biomed Mater Res 1999;47:292–300.
21. Klyscz T, Jünger M, Jung F, Zeintl H: [Cap image—a new kind of computer-assisted video image analysis system for dynamic capillary microscopy.] Biomed Tech (Berlin) 1997;42:168–175.
22. Harris AG, Leiderer R, Peer F, Messmer K. Skeletal muscle microvascular and tissue injury after varying durations of ischemia. Am J Physiol 1996;271: H2388–H2398.
23. Langer S, Born F, Harris AG, Hatz R, Biberthaler P, Messmer K. OPS imaging versus intravital fluorescent microscopy for microvascular studies in wounds. Ann Plast Surg 2002;48:646–653.
24. Nolte D, Zeintl H, Steinbauer M, Pickelmann S, Messmer K. Functional capillary density: an indicator of tissue perfusion? Int J Microcirc Clin Exp 1995;15:244–249.
25. Langer S, Biberthaler P, Harris AG, Steinau HU, Messmer K. *In vivo* monitoring of microvessels in skin flaps: introduction of a novel technique. Microsurgery 2001;21:317–324.
26. Menger MD, Pelikan S, Steiner D, Messmer K. Microvascular ischemia–reperfusion injury in striated muscle: significance of "reflow paradox." Am J Physiol 1992;263:H1901–H1906.
27. Lee H, Cusick RA, Browne F, Ho Kim T, Ma PX, Utsunomiya H, Langer R, Vacanti JP. Local delivery of basic fibroblast growth factor increases both angiogenesis and engraftment of hepatocytes in tissue-engineered polymer devices. Transplantation 2002;73:1589–1593.
28. Soker S, Machado M, Atala A. Systems for therapeutic angiogenesis in tissue engineering. World J Urol 2000;18:10–18.
29. Collier JH, Camp JP, Hudson TW, Schmidt CE. Synthesis and characterization of polypyrrole–hyaluronic acid composite biomaterials for tissue engineering applications. J Biomed Mater Res 2000;–50:574–584.
30. Pieper JS, Hafmans T, Van Wachem PB, Van Luyn MJ, Brouwer LA, Veerkamp JH, Van Kuppevelt TH. Loading of collagen–heparan sulfate matrices with bFGF promotes angiogenesis and tissue generation in rats. J Biomed Mater Res 2002;62:185–194.
31. Brey EM, King TW, Johnston C, McIntire LV, Reece GP, Patrick CW Jr. A technique for quantitative three-dimensional analysis of microvascular structure. Microvasc Res 2002;63:279–294.
32. Jamell GA, Hollsten DA, Hawes MJ, Griffin DJ, Klingensmith WC, White WL, Spirnak J. Magnetic resonance imaging versus bone scan for assessment of vascularization of the hydroxyapatite orbital implant. Ophthal Plast Reconstr Surg 1996;12:127–130.
33. Yang CF, Yasukawa T, Kimura H, Miyamoto H, Honda Y, Tabata Y, Ikada Y, Ogura Y. Experimental corneal neovascularization by basic fibroblast growth factor incorporated into gelatin hydrogel. Ophthalmic Res 2000;32:19–24.
34. Nolte D, Menger MD, Messmer K. Microcirculatory models of ischaemia–reperfusion in skin and striated muscle. Int J Microcirc Clin Exp 1995;15(Suppl 1):9–16.
35. Menger MD, Vajkoczy P, Beger C, Messmer K. Orientation of microvascular blood flow in pancreatic islet isografts. J Clin Invest 1994;93:2280–2285.
36. Beumer GJ, van Blitterswijk CA, Bakker D, Ponec M. A new biodegradable matrix as part of a cell seeded skin substitute for the treatment of deep skin defects: a physico-chemical characterisation. Clin Mater 1993;14:21–27.
37. Papadaki M, Mahmood T, Gupta P, Claase MB, Grijpma DW, Riesle J, van Blitterswijk CA, Langer R. The different behaviors of skeletal muscle cells and chondrocytes on PEGT/PBT block copolymers are related to the surface properties of the substrate. J Biomed Mater Res 2001;54:47–58.
38. Nor JE, Peters MC, Christensen JB, Sutorik MM, Linn S, Khan MK, Addison CL, Mooney DJ, Polverini PJ. Engineering and characterization of functional human microvessels in immunodeficient mice. Lab Invest 2001;81:453–463.